

Uniaxial tensile strain and exciton–phonon coupling in bent ZnO nanowires

Rui Chen,¹ Quan-Lin Ye,^{1,2} T. C. He,¹ T. Wu,^{1,a)} and H. D. Sun^{1,b)}

¹*Division of Physics and Applied Physics, School of Physical and Mathematical Sciences, Nanyang Technological University, Singapore 637371*

²*Department of Physics, Hangzhou Normal University, Hangzhou 310036, People's Republic of China*

(Received 29 April 2011; accepted 31 May 2011; published online 17 June 2011)

We investigate the optical property of bent ZnO nanowires (NWs) obtained by low energy argon ion milling. At room temperature, the bent NWs demonstrates an enhanced near band edge ultraviolet emission, while the deep level green emission is totally suppressed. Temperature dependent photoluminescence measurements were carried out between 10 and 300 K for both the as-grown and the bent ZnO NWs. It is found that the emission peak energy of the bent NWs systematically shifts to lower energy compared to the as-grown NWs in the whole measured temperature range. Our results indicate that the redshift in the emission peak is related to the uniaxial tensile strain and the enhanced exciton–phonon coupling strength in the bent ZnO NWs. © 2011 American Institute of Physics. [doi:10.1063/1.3601479]

One-dimensional (1D) semiconductor nanowires (NWs) have been the focus of current research due to the prospect as building blocks for nanotechnology.^{1–3} Wurtzite ZnO, a wide band gap (3.37 eV) polar semiconductor with a large exciton binding energy of 60 meV, has significant advantages on its potential application in short wavelength optoelectronic devices.⁴ Unfortunately, the room temperature emission from ZnO NWs always display a broad deep level emission (DLE) in the green region along with the weak near band edge emission in the ultraviolet (UV) region.⁵ In order to advance the practical applications, various surface modifications such as plasma immersion ion implantation,⁶ polymer passivation,⁷ surface plasmon,⁸ and hydrogen plasma treatment,⁹ have been successfully employed to enhance the UV emission of as-grown ZnO NWs.

It is known that strain is a useful method for modulating the physical properties of semiconductor. Especially, advanced transistors benefit from the enhanced mobility in strained silicon.¹⁰ In previous investigations, strain has been used successfully to modify the optical and electrical properties of ZnO NWs.^{11–13} However, up till now, the bending deformation of ZnO NWs is elastic in nature, that is, the bending of the NWs is due to the adhesion and friction forces between NWs and substrate, and the bent NW will recover to its straight shape if separated from the substrate.¹¹ Therefore, the derived properties are volatile, which hinders wide spread applications. There is relatively less effort devoted to inelastic bent ZnO NWs, which should be able to maintain its superiority for the application in multifunctional devices.

There are limited routes toward bent NWs.¹⁴ Argon ion (Ar⁺) milling technique is considered to be an effective surface modification technique due to its inexpensive and high-throughput. In this letter, we demonstrate the inelastic bending of ZnO NWs using low energy Ar⁺ milling. The optical properties of the ZnO NWs before and after bending were comparatively investigated. It was found that the Ar⁺ milling effectively quenched the DLE of ZnO, and the UV emission was enhanced due to surface modification. The bending de-

formation not only introduces uniaxial tensile strain but also enhances the exciton–phonon coupling, which results in a redshift in the peak emission compared to the as-grown ZnO NWs.

The samples were fabricated on sapphire substrates using a vapor transport method.^{15,16} To produce bent ZnO NWs, Ar⁺ milling treatments were carried out in a high vacuum chamber equipped with an ion source. During the one minute milling process, the ion beam energy was fixed at 630 eV with a beam current of 50 mA and an acceleration voltage of 300 V. The angle between the ion beam and the surface normal was systematically adjusted to optimize the bending results. Subsequent photoluminescence (PL) measurements were performed between 10 and 300 K within a closed cycle helium cryostat.¹⁷ A cw He–Cd laser emitting at 325 nm was used as the PL excitation source and the signal was dispersed by a 750 mm monochromator combined with suitable filters, and detected by a photomultiplier using the standard lock-in amplifier technique.

Figures 1(a) represents the schematic diagrams of the process flow to achieve bent ZnO NWs. Typical field emission scanning electron microscope (FESEM) image of the

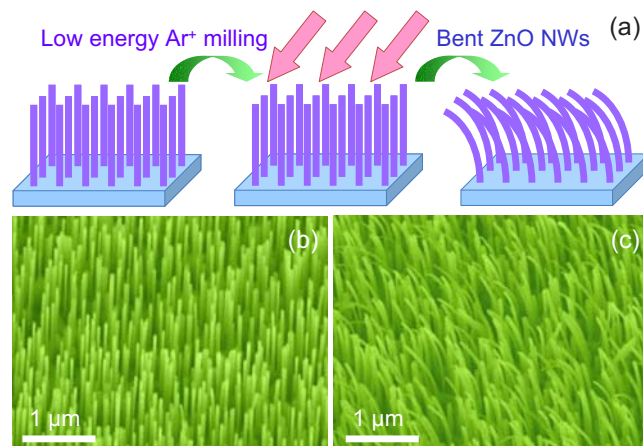


FIG. 1. (Color online) (a) Schematic diagrams show the bent ZnO NWs obtained by low energy Ar⁺ milling. (b) and (c) represent the FESEM image of the ZnO NWs before and after bending.

^{a)}Electronic mail: tomwu@ntu.edu.sg.

^{b)}Electronic mail: hdsun@ntu.edu.sg.

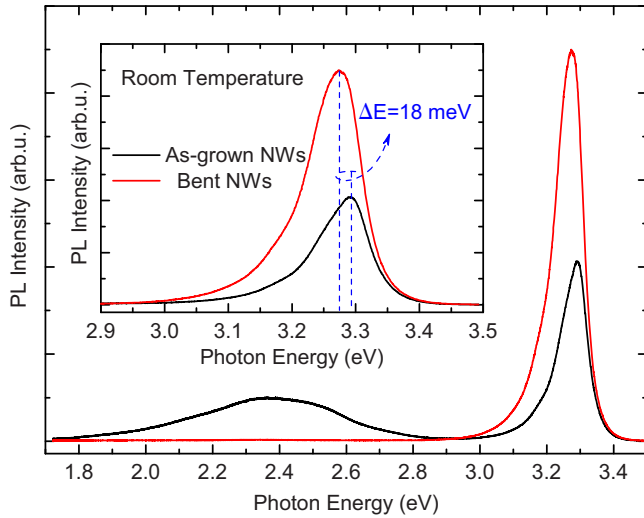


FIG. 2. (Color online) Room temperature PL spectrum of the ZnO NWs before and after bending. The inset shows the close-up image of the PL spectrum in the high energy region.

as-grown ZnO NWs is shown in Fig. 1(b), displaying high-density vertically aligned ZnO NWs arrays. The x-ray diffraction result (not shown here) indicates that the ZnO NWs are grown with a c-axis orientation. After the milling process, ZnO NWs were found to transform from straight to bent, as shown in Fig. 1(c). It is interesting to note that the bending deformation is inelastic, which is different from the previous reports.^{11,13}

Figure 2 displays the room temperature PL spectrum of the ZnO NWs before and after bending. The strong near band edge emission compared to the DLE from as-grown NWs suggests that the sample has high crystalline quality. It is noted that after bending, the visible DLE is totally suppressed, while the UV emission is enhanced by a factor of ~ 2.2 . The reason of this can be ascribed to passivation of the surface hole and electron trapping sites during low energy Ar⁺ milling.⁶ From the close-up PL spectrum shown in the inset of Fig. 2, it can be seen that the near band edge emission from bent ZnO NWs is located at 3.273 eV, with a redshift of 18 meV compared to the as-grown ZnO NWs positioned at 3.291 eV. The redshift in the PL emission at room temperature could be due to various reasons such as laser heating effect, presence of uniaxial stress/strain, and the different contributions of excitonic emission and their phonon replicas.¹⁸ However, the PL measurements were performed under similar conditions, and the laser power density was low (~ 5 mW/cm²) for the measurements. Therefore, the laser heating effect can be ruled out.

To investigate the optical property of ZnO NWs after bending, temperature dependent PL measurement was carried out. As shown in Fig. 3(a), the as-grown ZnO NWs at 10 K are dominated by excitonic emission at 3.355 eV, originating from the radiative recombination of neutral donor-bound excitons (D⁰X). Two strong peaks at 3.359 and 3.366 eV are assigned to recombination of donorlike surface excitons (SXs).¹⁹ One more shoulder can be observed which is related to recombination of free exciton (FX) at 3.374 eV. Comparing to the as-grown sample, bent ZnO NWs demonstrates similar D⁰X emission. However, a suppression of the SX emission can be clearly observed, which can be related to the modification of surface trapping sites located near the

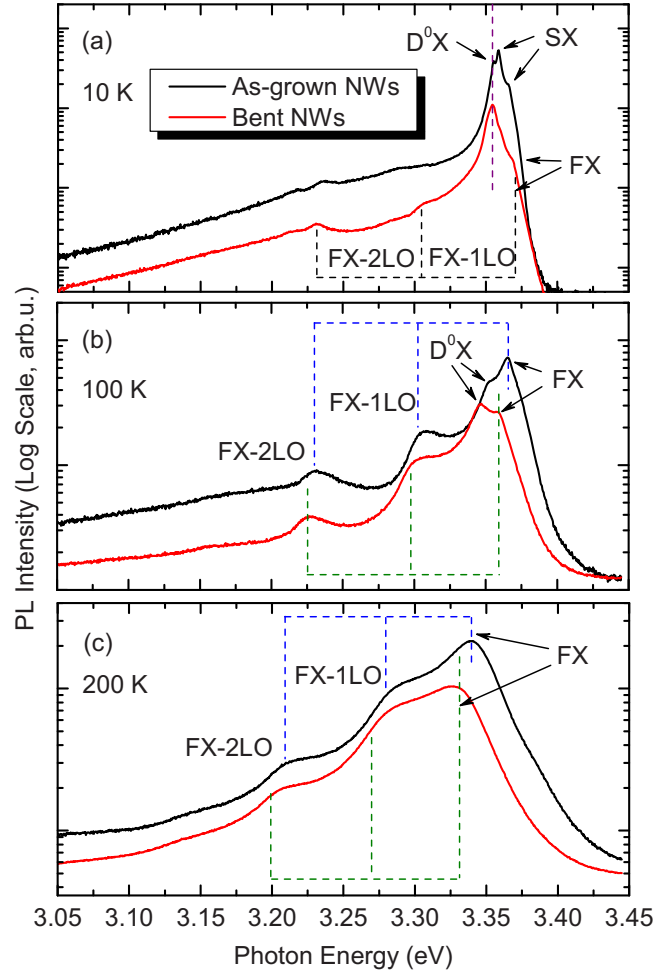


FIG. 3. (Color online) Comparative PL spectrum of the ZnO NWs before and after bending at various temperatures. All the curves are shifted vertically for better comparison.

surface of the sample. At the high energy region, a peak ~ 3.369 eV from FX emission can be observed, with longitudinal-optical (LO) phonon replica served at low energy side of the spectra. A closer look at the peak position of FX emission reveals that the bent ZnO NWs show a slightly redshift compared to the as-grown sample. This phenomenon is also verified by PL spectrum at higher temperatures as shown in Figs. 3(b) and 3(c). It is interesting to note that emissions including D⁰X, FX, and the related LO phonon replicas shifted to lower energy after bending. In ideal case, the bent NWs will suffer both tensile and compressive strain at the outer and inner edges, respectively. However, it is known that the strain distribution is very sensitive to materials and loading conditions. Based on the measurement results, we can claim that local tensile strain is the dominated uniaxial stress in our bent ZnO NWs.

Thermal shift in the band gap of semiconductors is related to the thermal dilation of the crystal lattice as well as electron-phonon interactions.²⁰ The temperature dependence of this characteristic can be well described by the following model proposed by Manoogian and Woolley (MW),²¹

$$E(T) = E(0) + UT^S + V\theta[\coth(\theta/2T) - 1], \quad (1)$$

where $E(0)$ is the band gap at $T=0$ K, U is the lattice dilation coefficient, S describes the average exciton-phonon coupling strength, V is the temperature-dependent shift in the

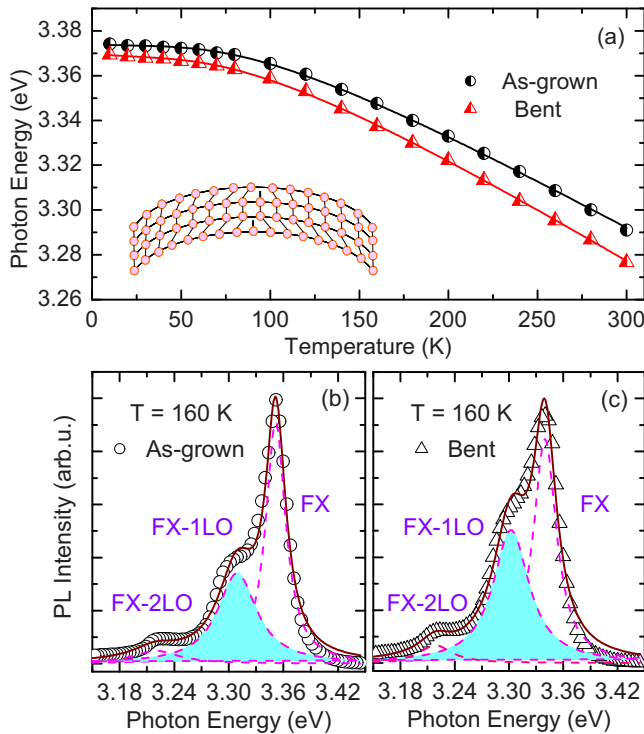


FIG. 4. (Color online) (a) Temperature dependent peak position of the ZnO NWs before and after bending. Inset shows the creation of dangling bonds at the outer surface of the bent NW. [(b) and (c)] The PL spectrum at 160 K for the two samples fitted with multi-Lorentzian function. The area from the contribution of FX-1LO is filled.

band gap, and θ is the temperature-related parameter. Figure 4(a) presents the emission peak of FX as a function of temperature. The parameters extracted from the fitting are summarized in Table I. The obtained values are in good agreement with the reported data.²² As can be seen from Fig. 4(a), the peak position of the bent ZnO NWs always demonstrates a redshift compared to the as-grown sample as discussed above. Moreover, it is noted that the peak energy difference between two samples increases with increasing temperature. This feature is due to the increase in S value which can be revealed from Table I. The statement is further confirmed by fitting the 160 K PL spectrum of the two samples with three Lorentzian functions, which determines the contribution of FX and the phonon replicas. Figures 4(b) and 4(c) provide the information that the relative contribution of FX-1LO with respect to FX emission in the bent ZnO NWs is larger than that of the as-grown sample. The relative higher amplitude of the FX-LO emission indicates that the exciton-phonon coupling strength is enhanced after bending.

As a polar semiconductor, ZnO experiences a strong Fröhlich interaction (FI) that results in the exciton-phonon interaction. However, it was found that the FI is extremely small in a perfect crystal due to parity conservation.²³ Nevertheless, this rule can be broken in the case of NWs due to

TABLE I. Parameters obtained from MW fitting for the two samples.

ZnO NWs	$E(0)$ (eV)	U ($\times 10^{-5}$ eV/K ⁵)	S	V ($\times 10^{-4}$ eV/K)	θ (K)
As-grown	3.3739	-3.00	0.90	-2.20	300
Bent	3.3695		1.09		

the larger surface-to-volume ratio, especially for the case of bent ZnO NWs discussed herein. As shown in the inset of Fig. 4(a), there exist some dangling bonds located at the outer and inner edges of the bent NWs due to the inelastic bending deformation. It is expected that the crystal imperfection will give rise to additional intermediate states which enhance the exciton-phonon coupling strength.²³ This has been investigated for ZnO, where the relative intensity of the FX-1LO line increased for the sample with higher defect densities.¹⁸

In summary, we have demonstrated the inelastic bending of ZnO NWs through low energy Ar⁺ milling. It was found that the peak position of the bent ZnO NWs demonstrates a redshift with respect to the as-grown sample at various temperatures. Moreover, the peak energy difference between the two samples increases with temperature. Our data revealed that both uniaxial tensile strain and an enhanced exciton-phonon coupling strength are responsible to the optical property change in the bent ZnO NWs. This approach toward inelastically bent NWs arrays should be applicable to other 1D nanomaterials and find application in advanced devices.

- ¹X. Wang, C. J. Summers, and Z. L. Wang, *Nano Lett.* **4**, 423 (2004).
- ²R. Chen, M. I. Bakti Utama, Z. Peng, B. Peng, Q. Xiong, and H. D. Sun, *Adv. Mater. (Weinheim, Ger.)* **23**, 1404 (2011).
- ³Y. Xia, P. Yang, Y. Sun, Y. Wu, B. Mayers, B. Gates, Y. Yin, F. Kim, and H. Yan, *Adv. Mater. (Weinheim, Ger.)* **15**, 353 (2003).
- ⁴R. Chen, B. Ling, X. W. Sun, and H. D. Sun, *Adv. Mater. (Weinheim, Ger.)* **23**, 2128 (2011).
- ⁵R. Chen, Y. Y. Tay, J. Ye, Y. Zhao, G. Z. Xing, T. Wu, and H. D. Sun, *J. Phys. Chem. C* **114**, 17889 (2010).
- ⁶Y. Yang, X. W. Sun, B. K. Tay, P. H. T. Cao, J. X. Wang, and X. H. Zhang, *J. Appl. Phys.* **103**, 064307 (2008).
- ⁷K. W. Liu, R. Chen, G. Z. Xing, T. Wu, and H. D. Sun, *Appl. Phys. Lett.* **96**, 023111 (2010).
- ⁸K. W. Liu, Y. D. Tang, C. X. Cong, T. C. Sum, A. C. H. Huan, Z. X. Shen, W. Li, F. Y. Jiang, X. W. Sun, and H. D. Sun, *Appl. Phys. Lett.* **94**, 151102 (2009).
- ⁹C.-C. Lin, H.-P. Chen, H.-C. Liao, and S.-Y. Chen, *Appl. Phys. Lett.* **86**, 183103 (2005).
- ¹⁰D. Shiri, Y. Kong, A. Buin, and M. P. Anantram, *Appl. Phys. Lett.* **93**, 073114 (2008).
- ¹¹X. Han, L. Kou, X. Lang, J. Xia, N. Wang, R. Qin, J. Lu, J. Xu, Z. Liao, X. Zhang, X. Shan, X. Song, J. Gao, W. Guo, and D. Yu, *Adv. Mater. (Weinheim, Ger.)* **21**, 4937 (2009).
- ¹²B. Yan, R. Chen, W. W. Zhou, J. X. Zhang, H. D. Sun, H. Gong, and T. Yu, *Nanotechnology* **21**, 445706 (2010).
- ¹³C. P. Dietrich, M. Lange, F. J. Klupfel, H. von Wenckstern, R. Schmidt-Grund, and M. Grundmann, *Appl. Phys. Lett.* **98**, 031105 (2011).
- ¹⁴Y. Shen, J.-I. Hong, S. Xu, S. Lin, H. Fang, S. Zhang, Y. Ding, R. L. Snyder, and Z. L. Wang, *Adv. Funct. Mater.* **20**, 703 (2010).
- ¹⁵X. Wang, G. Li, T. Chen, M. Yang, Z. Zhang, T. Wu, and H. Chen, *Nano Lett.* **8**, 2643 (2008).
- ¹⁶Z. Zhang, J. B. Yi, J. Ding, L. M. Wong, H. L. Seng, S. J. Wang, J. G. Tao, G. P. Li, G. Z. Xing, T. C. Sum, C. H. Alfred Huan, and T. Wu, *J. Phys. Chem. C* **112**, 9579 (2008).
- ¹⁷R. Chen, G. Z. Xing, J. Gao, Z. Zhang, T. Wu, and H. D. Sun, *Appl. Phys. Lett.* **95**, 061908 (2009).
- ¹⁸C. H. Ahn, S. K. Mohanta, N. E. Lee, and H. K. Cho, *Appl. Phys. Lett.* **94**, 261904 (2009).
- ¹⁹L. Wischmeier, T. Voss, I. Rückmann, J. Gutowski, A. C. Mofor, A. Bakin, and A. Waag, *Phys. Rev. B* **74**, 195333 (2006).
- ²⁰R. Chen, D. Li, B. Liu, Z. Peng, G. G. Gurzadyan, Q. Xiong, and H. D. Sun, *Nano Lett.* **10**, 4956 (2010).
- ²¹A. Manooogian and J. C. Woolley, *Can. J. Phys.* **62**, 285 (1984).
- ²²D. W. Hamby, D. A. Lucca, M. J. Klopstein, and G. Cantwell, *J. Appl. Phys.* **93**, 3214 (2003).
- ²³T. Voss, C. Bekeny, L. Wischmeier, H. Gafsi, S. Borner, W. Schade, A. C. Mofor, A. Bakin, and A. Waag, *Appl. Phys. Lett.* **89**, 182107 (2006).